THE JOURNAL OF PHYSICAL CHEMISTRY B

Article

pubs.acs.org/JPCB

Oxidation Mechanism of Methionine by HO• Radical: A Theoretical Study

Tiziana Marino,*[,†] Catalina Soriano-Correa,[†,‡] and Nino Russo[†]

[†]Dipartimento di Chimica, Università della Calabria, I-87030 Arcavacata di Rende, Italy

[‡]Química Computacional. FES-Zaragoza, Universidad Nacional Autónoma de México (UNAM), C.P. 09230 Iztapalapa, México, D.F., Mexico

ABSTRACT: A theoretical investigation at the MP2/6-311++G(2d,2p)//MP2/6-31+G(d,p) level was employed in order to study the one-electron oxidation mechanism of methionine in aqueous solution. Three reaction paths corresponding to the HO•, O_2 attack and hydrolysis were considered. Results show that all the processes are exothermic and that the rate determining step can be associated with the hydrolysis reaction. DFT computations with different exchange-correlation potentials were performed in order to verify their reliability in the description of the cyclic adduct produced in the HO• attack step.

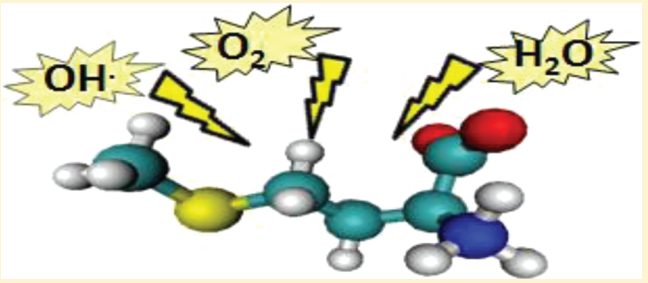

INTRODUCTION

The oxidation of methionine in peptides and proteins represents an important target of numerous reactive oxygen species (ROS).[1,2] In fact, depending on the nature of the oxidizing species, methionine can undergo two-electron oxidation (like HOCl, $^1O_2$, H_2O_2, ROOH, and $ONOO^-$/ONOOH) to give sulfoxides or one-electron oxidation (like RS•, HO•, RO•, $CO_3^{-•}$, N_3•, and ROO•) to give methionine radical cations.[3] Under conditions of oxidative stress,[1−3] the methionine oxidation can be implicated in the development and progression of neurodegenerative diseases (e.g., Alzheimer's and Parkinson's) as well as in the aging processes.[4−6] In particular, Met35 in amyloid β-peptide(25−35) seems to be involved in the aggregation, neurotoxicity, and radical generation. Replacing this residue with NLeu, Lys, Leu, and Tyr, amino acids without a sulfur atom in the side chain, removes the oxidative stress and neurotoxic properties of the peptide, confirming the key role of the methionine in Alzheimer's disease.[7]

In the past, radiation chemistry of sulfur compounds and, in particular, of methionine, was studied extensively.[8−12] In general, hydroxyl radicals and other one-electron oxidants can react with dialkyl sulfides following a complex sequence of reactions.[13,14]

In particular, Asmus et al. stated, by using radiation chemical methods (ns−ms pulse radiolysis), that the reaction of HO• radical with methionine generates a stable intramolecular S∴N-bonded five-member radical cation that, subsequently, by decarboxylation (nearly 90% yield at pH 7) forms a 3-methyl thiol propyl amino radical.[8]

The same authors in a subsequent work[9] performed on the above-mentioned reaction in water found that the initial step is a competition process between addition of HO• radical to the sulfur atom (∼90%) and hydrogen abstraction (∼10%).

In the past decade, pulse radiolysis combined with quantum chemical methods, which are gaining increasing importance, have proven useful in the elucidation of the oxidation reaction mechanism of different chemical sulfur containing species.[15−17]

Previous theoretical model calculations focused on oxidation of methionine and their derivatives have justified the presence of a S∴N three-electron bonded radical species.[18−22] Recently, Galano et al. have performed a density functional study useful to obtain activation energies and rate constants for methionine + OH radical in the gas phase taking into account only the hydrogen abstraction reaction from methionine.[23]

Most recently, Barata-Vallejo and co-workers investigated the reaction of HO• and H• radicals generated by γ-radiolysis of methionine in water solvent in the absence and presence of molecular oxygen.[24]

Although these theoretical and experimental works exist, qualitative and quantitative information on the whole mechanism of Met oxidation by HO• radical in aqueous solution is scarce. Thus, the purpose of the present theoretical study, performed at the MP2 level, is to provide new insight on this important reaction.

COMPUTATIONAL METHODS

All the computations were performed with the Gaussian 09 (G09) suite of programs.[25]

Full optimizations without any symmetry restriction were carried out at the second-order Möller-Plesset perturbation theory (MP2) level[26] with the 6-31+G(d,p) basis set. On the basis of these optimized geometries, single-point calculations

Received: January 2, 2012
Revised: April 12, 2012
Published: April 21, 2012

   dx.doi.org/10.1021/jp3000398 | J. Phys. Chem. B 2012, 116, 5349−5354

Scheme 1

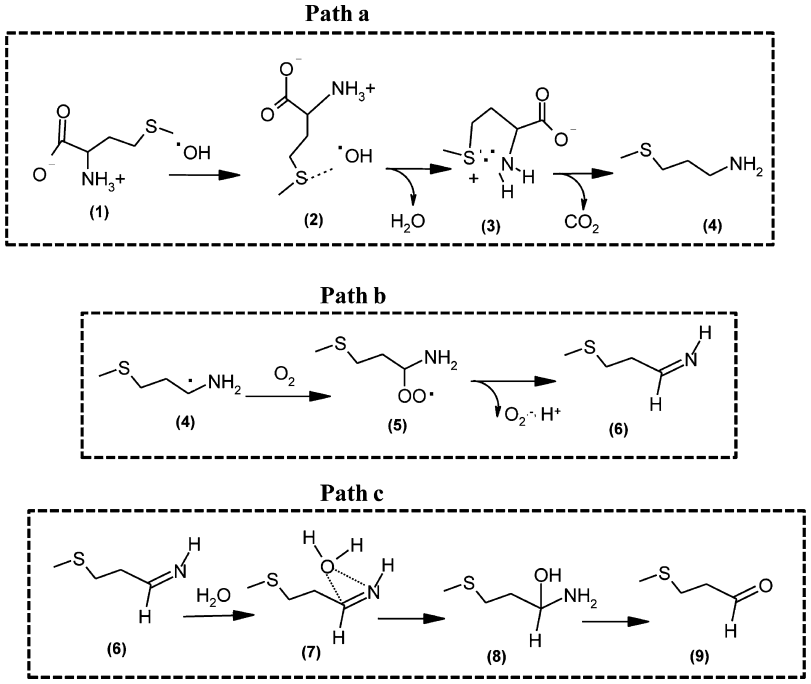

with the 6-311++G(2d,2p) larger basis set were done in order to obtain more accurate energies. All the calculations were performed in aqueous medium where the methionine exists as the zwitterion form. Solvent effects were described through a continuum approach by means of the IEF version of the polarizable continuum model (PCM)[27−30] as implemented in G09. At this purpose, the dielectric constant of water (ε = 80) was employed to simulate the surroundings media where the studied reaction occurs.

Vibrational frequencies were calculated on each optimized structure at the same level of theory of the optimizations, and zero point vibrational corrections were added to final ΔG energies.

A net charges distribution was obtained using the natural population analysis (NPA) method.[31−33] Moreover, analysis of natural bonding orbitals (NBO) was used to estimate the nature of the bonds within studied systems.

Further calculations based on density functional theory (DFT) were performed in order to establish which functional is reliable to describe the three-electron bond characterizing species **3**. For this species, geometry optimization was performed by using different hybrid and meta-hybrid exchange-correlation potentials (B3LYP,[34−36] BHandH,[37,38] BHHLYP,[35,37] PBE1PBE,[39] M06 and M06-2x[40]).

RESULTS AND DISCUSSION

On the basis of the indications arising from previous works,[8−14,24] we have studied the whole reaction mechanism of the addition of HO$^\bullet$ radical to methionine (**Met**, **1**) (see Scheme 1) at the MP2 level. As suggested by the experimental evidence,[24] the formation of the corresponding sulfoxide compound was neglected, since it represents a minor reaction channel in the HO$^\bullet$ radical attack to methionine.

The first and second steps of path **a** (Scheme 1) were the object of previous theoretical investigations at different levels of theory.[20,22,23] The step relative to the formation of species **2** can generate different adducts (e.g., HO$^\bullet$ can approach the sulfur atom or the CH_2 carbon chain), and for this reason, preliminary calculations were performed to establish the most stable one. Three adducts (**2**, **2a**, and **2b** of Figure 1) were

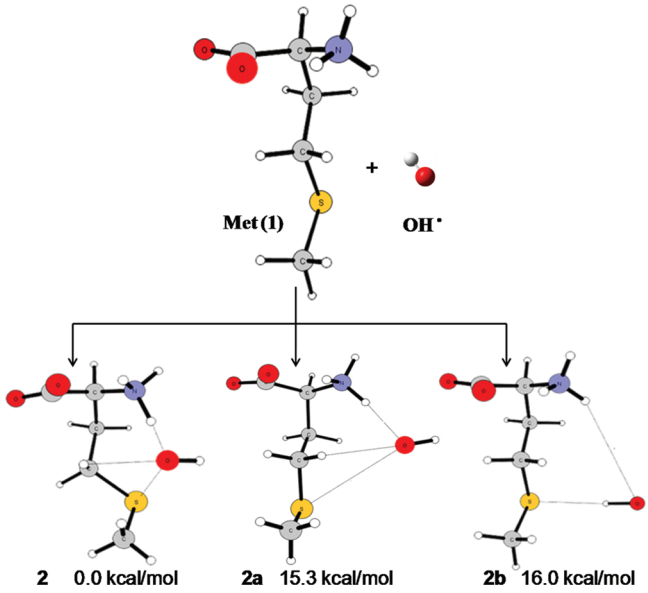

Figure 1. MP2/6-31+G(d,p) optimized structures for the three adducts obtained by HO$^\bullet$ attack to zwitterion form of **Met** (**1**).

localized into an energetic range of 16 kcal/mol. They essentially differ in the orientation of the hydroxyl group, and the structure of adduct **2** resulted in being the lowest minimum. None of the obtained structures is the HO$^\bullet$ adduct at sulfur, since during the optimization the HO$^\bullet$ reaches different positions around the Met . In the less stable radical (**2b**, 16.0 kcal/mol above **2**), the HO$^\bullet$ interacts with the sulfur atom though an H-bond (2.88 Å), while in the other one (**2a**, 15.3 kcal/mol above **2**) it is oriented toward the ammonium group with the formation of a H-bond (1.88 Å) (see Figure 1).

dx.doi.org/10.1021/jp3000398 | J. Phys. Chem. B 2012, 116, 5349−5354

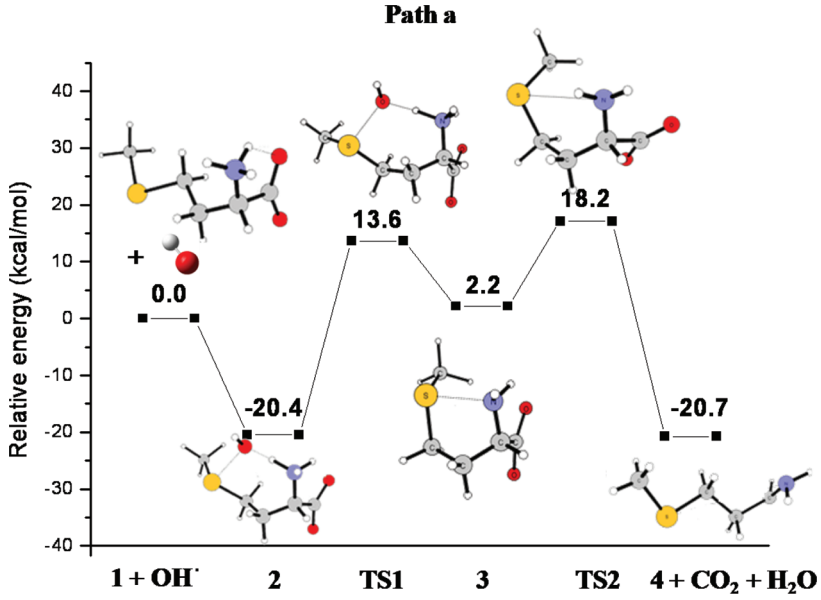

Figure 2. MP2/6-311++G(2d,2p)//MP2/6-31+G(d,p) PES of path **a**.

On the basis of previous results, structure **2** (Figure 1) was consequently considered as an adduct in path **a** of the addition of HO• radical to methionine. The potential energy surface (PES) for this reaction path is depicted in Figure 2. From this figure, it is evident that the addition of HO• radical to the zwitterion form of **Met** gives rise to adduct **2** without an energy barrier and with a stabilization energy (with respect to the separated reactants) of about 20.4 kcal/mol.

From the geometrical point of view, radical species **2** is a quasi-cyclic structure stabilized by the bridging OH group that forms a strong H-bond (1.53 Å) with the amine N−H and a long-range interaction with the sulfur (2.17 Å). In this way, the hydroxyl group is ready to take up a proton from the ammonium group, so a H_2O molecule can be eliminated, leaving **Met** radical cation with $-NH_2$ group, as described by the next step. The peculiar arrangement of HO• in the Met (species **2**) can give an explanation for the lack of the product Met(O) as observed in the aliphatic sulfides.[12,20,41−43] Species **2** is an example of the possible role played by the neighboring groups on the stabilization of the radical species.

The transition state **TS1** describes the proton transfer from the nitrogen atom of the amine moiety (1.17 Å) to the oxygen of the hydroxyl group (1.34 Å), leading to the formation of a water molecule (see Figure 2). An evident geometrical difference with respect to the previous minimum is given by the distance S−N that is 3.63 Å in **TS1** versus 3.90 Å in adduct **2**. The imaginary frequency (ν_i = 60.1 cm^{-1}) is associated with the stretching O−H. After overcoming **TS1**, species **3** is obtained. This structure, similar to a five-member ring, was experimentally detected and characterized by UV spectroscopy[24] and previously predicted by theory in methionine methyl ester.[20] NBO analysis of this intermediate indicates a partial covalent interaction between sulfur and nitrogen atoms. This S−N bond (2.45 Å) has a bond order of 0.222 and is obtained by the overlap of the hybrid s(8.71%)p(91.29%) and s(2.70%)-p(96.88%)d(0.42%) orbitals of N and S, respectively. The values of natural charges (−0.219 and 0.672 e for N and S, respectively) suggest that, owing to the nature radical cation of adduct **3**, a charge transfer from S to N occurs.

Looking at the potential energy profile (Figure 2), we note that adduct **3** is very close in energy to the reactants (−2.2 kcal/mol). This is indicative of a weak σ bond (-S--N-) as evidenced by the NBO analysis. Our findings support what was obtained by previous works carried out on similar sulfur containing systems.[8,12,20,22]

Due to the peculiarity of this interaction, we have performed a benchmark by using different exchange-correlation potentials in order to verify if the DFT based methods are able to correctly describe this kind of interaction. The main results are collected in Figure 3. From these calculations, it can be evinced

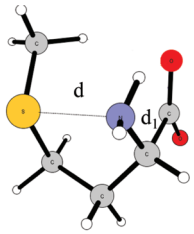

Å	MP2	B3LYP	BHandH	BHHLYP	PBE1PBE	M06	M06-2x
d	2.449	3.355	2.429	2.489	2.524	3.372	2.490
d_1	1.569	3.297	1.548	1.566	1.574	2.957	1.578

Figure 3. MP2 and DFT main optimized geometrical parameters for adduct **3**.

how B3LYP and M06 are not able to describe this kind of bond. In fact, with these exchange-correlation potentials, species **3** is not stable and undergoes a spontaneous decarboxylation generating directly the α-aminoalkyl radical **4** weakly bonded to the CO_2. All other exchange-correlation potentials used are able to describe **3** as a minimum, and the N−S distance is similar to that obtained at the MP2 level. In particular, the BHandH potential gives a distance of 2.43 Å very close to the MP2 value (2.45 Å).

The intermediate **3** can lose the CO_2 group, giving the α-aminoalkyl radical **4** that lies at 20.8 kcal/mol below the

dx.doi.org/10.1021/jp3000398 | J. Phys. Chem. B 2012, 116, 5349−5354

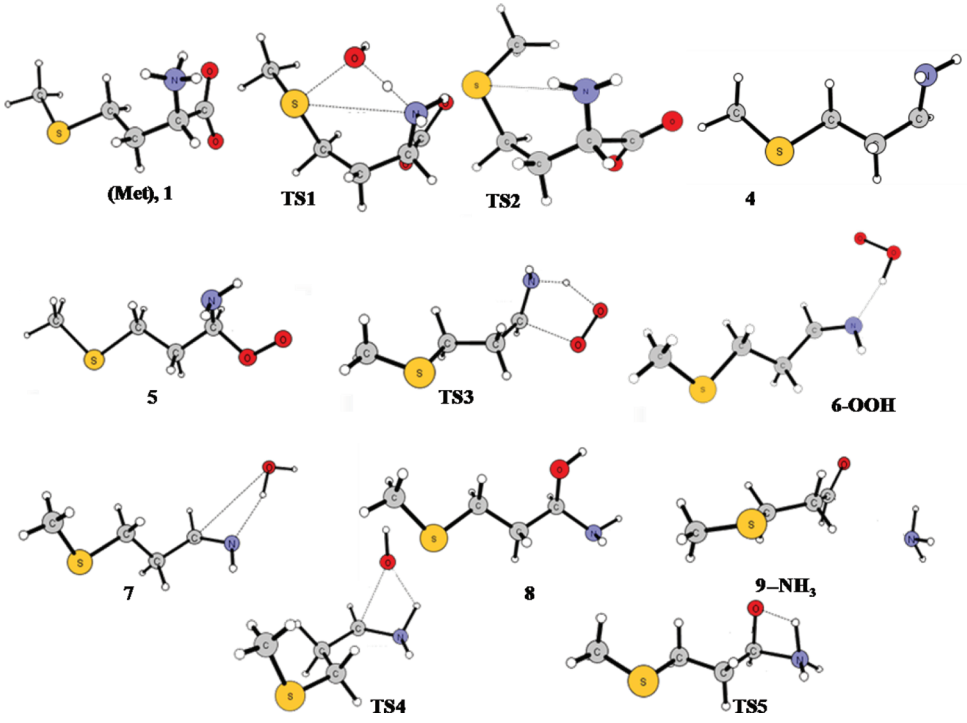

Figure 4. MP2/6-31+G(d,p) optimized structures of all the minima and maxima of paths **a**, **b**, and **c**.

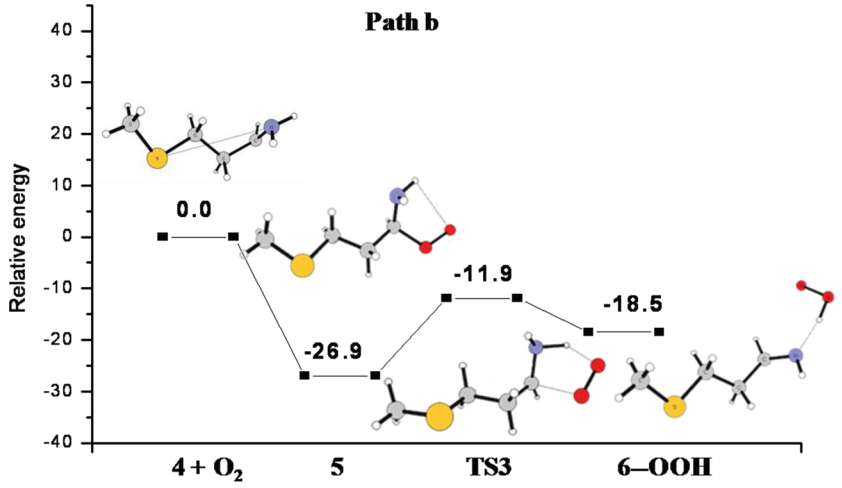

Figure 5. MP2/6-311++G(2d,2p)//MP2/6-31+G(d,p) PES of path **b**.

reactant energies. This step requires 16.0 kcal/mol, as indicated by the presence of transition state **TS2**. In this stationary point, the CO_2 moiety lies at 1.62 Å from the α-carbon and the relative imaginary frequency (ν_i = 981.7 cm^{-1}) clearly describes the stretching mode of the C−C bond between the α-carbon and the carbon of CO_2. The product **4** shows an extended chain even if the radical amine moiety assumes a cis orientation (see Figure 2). Our PES for path **a** (see Scheme 1) confirms that the N-oxidation (described by the formation of species **3**) and decarboxylation (described by species **4**) represent two independent consecutive processes, as already hypothesized by Hiller et al.[8] Considering the computed PES, it is possible to suggest that for this path the rate limiting step should be the HO radical addition.

Barata Vallejo et al.[24] observed that in three different experimental conditions, in solutions saturated by N_2O/O_2 (90:10) or by air N_2/O_2 (80:20) or by pure O_2, the consumption of Met can lead to the formation of different products. The major product isolated and identified by spectroscopic means was the aldehyde **9** (Scheme 1, path **c**), so our theoretical investigation was extended to the transformation of **4** into species **6** (path **b** of Scheme 1) that proceeds toward the final aldehyde **9** by path **c** (Scheme 1). The optimized geometries of the species are collected in Figure 4. The PES relative to path **b** is reported in Figure 5.

The addition of molecular oxygen at species **4** gives rise to the α-peroxy-amino radical **5** (Figures 4 and 5). Also in this case, as previously observed for species **2**, the addition process occurs without a transition state. Adduct **5** lies at −26.9 kcal/mol with respect to the separated reactants (species **4** + O_2).

The optimized structure of **5** shows that the molecular oxygen has attacked the α-carbon and its orientation points toward the amine hydrogen (O--H = 2.56 Å). The activation of the molecular oxygen is evident by looking at the O−O

dx.doi.org/10.1021/jp3000398 | J. Phys. Chem. B 2012, 116, 5349−5354

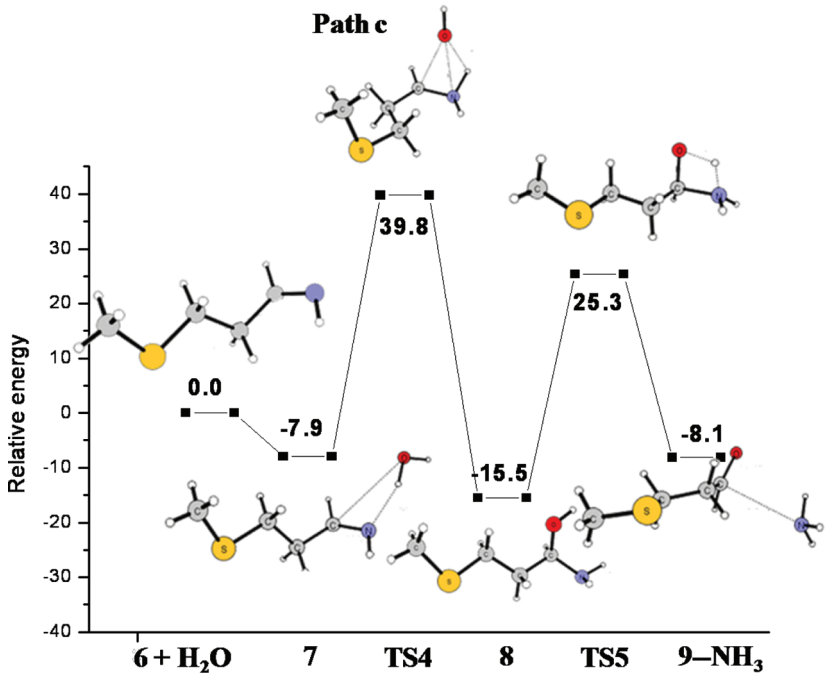

Figure 6. MP2/6-311++G(2d,2p)//MP2/6-31+G(d,p) PES of path **c**.

distance that is larger than in the isolated O_2 (1.31 Å versus 1.20 Å).

The reaction proceeds with the amine nitrogen that approaches the O_2 group, giving the final product **6** with the loss of HO_2•. This step requires an energy of 15.1 kcal/mol, as suggested by **TS3** in which, in a concerted way, the rotation of the amino moiety and the proton shift to the oxygen causes the breaking of the O−Cα bond.

The **TS3** imaginary vibrational frequency (482 cm^{-1}) corresponds to these motions. The adduct **6**--OOH is more stable by about 18 kcal/mol than the reactants, and the NBO analysis clearly evidences a double bond that characterizes species **6** as an imine. As is evident from the PES reported in Figure 5, this step is fast, since all the species individuated along the PES lie below the reactant energies.

The last part of the reaction corresponding to the conversion of imine **6** into aldehyde **9** occurs throughout the hydrolysis (path **c** of Scheme 1). The computed PES is reported in Figure 6, while the optimized geometries of the intermediates as well as transition states are depicted in Figure 4. The hydrolysis takes place by a water molecule that generates the formation of adduct **7** in which the H_2O is linked to the nitrogen atom by a hydrogen bond (1.95 Å) and is stabilized with respect to the reactants of about 8 kcal/mol.

The reaction evolves through the **TS4** to a second intermediate, **8**, in which the OH group is linked to the Cα and the other water hydrogen is bonded to the nitrogen. The structure of **TS4** and the analysis of the relative imaginary frequency (547 cm^{-1}) clearly show the breaking of the O−H water bond. Consequently, from **8**, that lies at 15.5 kcal/mol with respect to the reactants, a proton shift from the OH hydrogen to the NH_2 group causes the loss of ammonia. The relative transition state (**TS5**) exhibited an imaginary frequency (1471.5 cm^{-1}) strictly related to the this proton shift involving oxygen (1.43 Å) and nitrogen (1.17 Å) atoms, that in turn generates the breaking of the C−N bond (1.56 Å). Looking at the reported PES, it is clear that the rate determining step for this path is dictated by the energy of **TS5**, while the entire process is exothermic by 8.1 kcal/mol.

CONCLUSIONS

The present study, performed at the MP2/6-311++G(2d,2p)//MP2/6-31+G(d,p) level, gave new insights to understand the reaction between HO• radical and methionine in aqueous solution and in the presence of molecular oxygen. The main conclusions derived from our work are summarized as follows:

- The oxidation can be described by three distinct and consecutive paths: OH radical attack, oxidation, and hydrolysis.
- The addition O_2 (path **b**) are characterized by a low energy barrier, while the other two require higher energies. The rate limited step for the entire reaction is determined by path **c** in which the hydrolysis process requires a major amount of energy.
- All the considered paths describe exothermic transformations.
- Contrarily to what was previously supposed, species **2** is not characterized by a HO^- location on the S atom, but its coordination is shared by more atoms. Probably this findings can justify the stability of this transient species.
- The formation of the critical adduct **3** and the decarboxylation process are two distinct processes, as experimentally supposed.
- NBO natural charge values on the S and N centers of adduct **3** confirm that for the decarboxylation a charge transfer from sulfur to the amino group is required.
- It was evidenced how B3LYP and M06, between the DFT potentials used, are not able to locate species **3** owing to the decarboxylation occurring without its formation.

AUTHOR INFORMATION

Notes

The authors declare no competing financial interest.

dx.doi.org/10.1021/jp3000398 | J. Phys. Chem. B 2012, 116, 5349−5354

■ ACKNOWLEDGMENTS

We gratefully acknowledge the Dipartimento di Chimica, Università della Calabria, for financial aid. Furthermore, the authors are grateful to Dirección General de Servicios de Cómputo Académico of the Universidad Nacional Autónoma de México for allocation of computer time in the KanBalam supercomputer and CASPUR (Rome) for the computer grand. C.S.-C. acknowledges financial support through DGAPA-UNAM and 0145086 CONACyT. Also, C.S.-C. wishes to thank the Dipartimento di Chimica, Università della Calabria, Italy, for the kind hospitality during her sabbatical stay.

■ REFERENCES

(1) Vogt, W. *Free Radical Biol. Med.* **1995**, *18*, 93−105.
(2) Stadtman, E. R.; Van Remmen, H.; Richardson, A.; Wehr, N. B.; Levine, R. L. *Biochim. Biophys. Acta* **2005**, *1703*, 135−140.
(3) Luo, S.; Levine, R. L. *FASEB J.* **2009**, *23*, 464−472.
(4) Schoneich, C. *Biochim. Biophys. Acta* **2005**, *1703*, 111−119.
(5) Schöneich, C. *Arch. Biochem. Biophys.* **2002**, *397*, 370−376.
(6) Moskovitz, J. *Biochim. Biophys. Acta* **2005**, *1703*, 213−219.
(7) Varadarajan, S.; Yatin, S.; Kanski, J.; Jahanshahi, F.; Allan, D. B. *Brain Res. Bull.* **1999**, *50*, 133−141.
(8) Hiller, K. O.; Masloch, B.; Göbl, M.; Asmus, K.-D. *J. Am. Chem. Soc.* **1981**, *103*, 2734−2743.
(9) Hiller, K. O.; Asmus, K.-D. *J. Phys. Chem.* **1983**, *87*, 3682−3688.
(10) Bonifačič, M.; Asmus, K.-D. *J. Chem. Soc., Perkin Trans 2* **1980**, 758−762.
(11) Hiller, K.-O.; Asmus, K.-D. *Int. J. Radiat. Biol.* **1981**, *40*, 583−595.
(12) Schöneich, C. F.; Aced, A.; Asmus, K. D. *J. Am. Chem. Soc.* **1993**, *115*, 11376−11383.
(13) Asmus, K.-D. In *Sulfur Centered Reactive Intermediates in Chemistry and Biology*, NATO, ASI Series, A: Life Sciences, Vol. 197; Chatgilialogu, C., Asmus, K.-D., Eds.; Plenum Press: New York, 1990; p 155.
(14) Asmus, K.-D. In *Radiation Chemistry: Present Status and Future Trends*; Jonah, C. D., Rao, B. S. M., Eds.; Elsevier: Amsterdam, 2001; p 341.
(15) Maity, D. K. *J. Am. Chem. Soc.* **2002**, *124*, 8321−8328.
(16) Maity, D. K. *J. Phys. Chem. A* **2002**, *106*, 5716−5721.
(17) Pogocki, D.; Serdiuk, K.; Schöneich, C. *J. Phys. Chem. A* **2003**, *107*, 7032−7042.
(18) Carmichael, I. *Acta Chem. Scand.* **1997**, *51*, 567−571.
(19) Fourré, I.; Bergès, J.; Braïda, B.; Houée-Levin, C. *Chem. Phys. Lett.* **2008**, *467*, 164−169.
(20) Shirdhonkar, M.; Maity, D. K.; Mohan, H.; Rao, B. S. M. *Chem. Phys. Lett.* **2006**, *417*, 116−123.
(21) Ji, W.-F.; Li, Z.-L.; Shen, L.; Kong, D.-X.; Zhang, H.-Yu. *J. Phys. Chem. B* **2007**, *111*, 485−489.
(22) Mishra, B.; Sharma, A.; Naumov, S.; Priyadarsini, K. I. *J. Phys. Chem. B* **2009**, *113*, 7709−7715.
(23) Galano, A.; Alvarez-Idaboy, R.; Crus-Torres, A.; Ruiz-Santoyo, M. E. *Int. J. Chem. Kinet.* **2003**, 212−221.
(24) Barata-Vallejo, S.; Ferreri, C.; Postigo, A.; Chatgilialoglu, C. *Chem. Res. Toxicol.* **2010**, *23*, 258−263.
(25) Frisch, M. J.; Trucks, G. W.; Schlegel, H. B.; Scuseria, G. E.; Robb, M. A.; Cheeseman, J. R.; Scalmani, G.; Barone, V.; Mennucci, B.; Petersson, G. A.; Nakatsuji, H.; Caricato, M.; Li, X.; Hratchian, H. P.; Izmaylov, A. F.; Bloino, J.; Zheng, G.; Sonnenberg, J. L.; Hada, M.; Ehara, M.; Toyota, K.; Fukuda, R.; Hasegawa, J.; Ishida, M.; Nakajima, T.; Honda, Y.; Kitao, O.; Nakai, H.; Vreven, T.; Montgomery, J. A., Jr.; Peralta, J. E.;Ogliaro, F.; Bearpark, M.; Heyd, J. J.; Brothers, E.; Kudin, K. N.; Staroverov, V. N.; Kobayashi, R.; Normand, J.; Raghavachari, K.; Rendell, A.; Burant, J. C.; Iyengar, S. S.; Tomasi, J.; Cossi, M.; Rega, N.; Millam, N. J.; Klene, M.; Knox, J. E.; Cross, J. B.; Bakken, V.; Adamo, C.; Jaramillo, J.; Gomperts, R.; Stratmann, R. E.; Yazyev, O.; Austin, A. J.; Cammi, R.; Pomelli, C.; Ochterski, J. W.; Martin, R. L.; Morokuma, K.; Zakrzewski, V. G.; Voth, G. A.; Salvador, P.; Dannenberg, J. J.; Dapprich, S.; Daniels, A. D.; Farkas, Ö.; Foresman, J. B.; Ortiz, J. V.; Cioslowski, J.; Fox, D. J. *Gaussian 09*, revision 02; Gaussian, Inc.: Wallingford, CT, 2009.
(26) Möller, C.; Plesset, M. S. *Phys. Rev.* **1934**, *46*, 618−622.
(27) Cancès, E.; Mennucci, B. *J. Math. Chem.* **1998**, *23*, 309−326.
(28) Cancès, E.; Mennucci, B.; Tomasi, J. *J. Chem. Phys.* **1997**, *107*, 3032−3041.
(29) Mennucci, B.; Cancès, E.; Tomasi, J. *J. Phys. Chem. B* **1997**, *101*, 10506−10517.
(30) Miertus, S.; Scrocco, E.; Tomasi, J. *J. Chem. Phys.* **1981**, *55*, 117−129.
(31) Foster, J. P.; Weinhold, F. *J. Am. Chem. Soc.* **1980**, *102*, 7211−7218.
(32) Reed, A. E.; Weinhold, F. *J. Chem. Phys.* **1983**, *78*, 4066−4703.
(33) Reed, A. E.; Weinstock, R. B.; Weinhold, F. *J. Chem. Phys.* **1985**, *83*, 735−746.
(34) Becke, A. D. *Phys. Rev. A: At., Mol., Opt. Phys.* **1988**, *38*, 3098−3100.
(35) Lee, C.; Yang, W.; Parr, R. G. *Phys. Rev. B: Condens. Matter Mater. Phys.* **1988**, *37*, 785−789.
(36) Stephens, P. J.; Devlin, F. J.; Chabalowski, C. F.; Frisch, M. J. *J. Phys. Chem.* **1994**, *98*, 11623−11627.
(37) Becke, A. D. *J. Chem. Phys.* **1993**, *98*, 1372−1377.
(38) Peréz-Jordá, J. M.; Becke, A. D. *Chem. Phys. Lett.* **1995**, *233*, 134−137.
(39) Adamo, C.; Barone, V. *J. Chem. Phys.* **1999**, *110*, 6158−6170.
(40) Zhao, Y.; Truhlar, D. G. *Theor. Chem. Acc.* **2008**, *120*, 215−241.
(41) Bobrowski, K.; Schöneich, C. *J. Chem. Soc., Chem. Commun.* **1993**, 795−797.
(42) Gawandi, V. B.; Mohan, H.; Mittal, J. P. *J. Phys. Chem. A* **2000**, *104*, 11877−11884.
(43) Bobrowski, K.; Holeman, J. *J. Phys. Chem.* **1989**, *93*, 6381−6387.